OFFICE OF NAVAL RESEARCH

GRANT: N00014-93-1-0331

TECHNICAL REPORT No. 74

96PRO-1032

The Oxidation State of Ni in the Nickel Oxide Electrode and Related Nickel Oxide Compounds: I. Spectroscopic Evidence

H. Sambe, T.M. Nabi, and D.E. Ramaker

Chemistry Department, George Washington University, Washington, D.C. 20052

A.N. Mansour

Naval Surface Warfare Center, 10901 New Hampshire Ave., Silver Spring, MD 20903

W.E. O'Grady

Surface Chemistry Branch, Naval Research Laboratory, Washington, D.C. 20375

Prepared for Publication in
Journal of Physical Chemistry

January 1997

REPORT DOCUMENTATION PAGE

Form Approved
OMB No. 0704-0188

1. AGENCY USE ONLY (Leave blank)	2. REPORT DATE	3. REPORT TYPE AND DATES COVERED
	1/97	Technical

4. TITLE AND SUBTITLE
The oxidation state of Ni in the nickel oxide electrode and related nickel oxide compounds: I. Spectroscopic Evidence

5. FUNDING NUMBERS
Grant #:
N00014-93-1-0331

6. AUTHOR(S)
H. Sambe, T.M. Nabi, and D.E. Ramaker
A.N. Mansour, W.E. O'Grady

7. PERFORMING ORGANIZATION NAME(S) AND ADDRESS(ES)
Department of Chemistry
The George Wahsington University
Washington, D.C. 20052

8. PERFORMING ORGANIZATION REPORT NUMBER
Technical Report
#74

9. SPONSORING/MONITORING AGENCY NAME(S) AND ADDRESS(ES)
Office of Naval Research
800 N. Quincy Street
Arlington, VA 22217-5000

10. SPONSORING/MONITORING AGENCY REPORT NUMBER
96PRO-1032

11. SUPPLEMENTARY NOTES

12a. DISTRIBUTION/AVAILABILITY STATEMENT
Approved for public release; distribution is unlimited.

12b. DISTRIBUTION CODE
Unlimited

13. ABSTRACT *(Maximum 200 words)*

The electronic structures of the nickel oxide electrode, $NiO_x(OH)_{2-x}$ for x=0-1.6, and related nickel oxide materials, Li-substituted NiO, $Li_yNi_{2-y}O_2$ for y=0-1 and "Ni^{4+}" compounds, $KNiO_2(IO_4)$ and $BaNiO_3$, have been investigated using Ni 2p XPS (X-ray photoemission spectroscopy) and Ni K-edge XAS (X-ray absorption spectroscopy) data. Three aspects of the Ni 2p XPS spectra (the main peak energy, satellite energy separation, and main-line shape) and three aspects of the Ni K-edge XAS spectra (pre-edge peak energy, K-edge energy at the half-step height, and white-line peak energy) have been analyzed by the aid of simplified models and theoretical calculations. The results of these analyses consistently favor the more covalent electronic structures, $Ni^{2+}O^{-}_x(OH)^{-}_{2-x}$ [x= 1.0 and 1.5], $Li^{+}Ni^{2+}O^{1.5-}_2$, $K^{+}Ni^{2+}O^{-}_2(IO_4)^{-}$ and $Ba^{2+}Ni^{2+}O^{1.33-}_3$, over the conventional ionic electronic structures, $Ni^{(2+x)+}O^{2-}_x(OH)^{-}_{2-x}$ [x= 1.0 and 1.5], $Li^{+}Ni^{3+}O^{2-}_2$, $K^{+}Ni^{4+}O^{2-}_2(IO_4)^{-}$ and $Ba^{2+}Ni^{4+}O^{2-}_3$. This finding suggests that the oxidation of the Ni^{2+} ion is harder than oxidation of the O^{2-} anion for these nickel oxide compounds studied here.

14. SUBJECT TERMS	15. NUMBER OF PAGES
Nickel Hydroxides, nickel electrode, XAFS, XPS	30
	16. PRICE CODE

17. SECURITY CLASSIFICATION OF REPORT	18. SECURITY CLASSIFICATION OF THIS PAGE	19. SECURITY CLASSIFICATION OF ABSTRACT	20. LIMITATION OF ABSTRACT
unclassified	unclassified	unclassified	unclassified

NSN 7540-01-280-5500

Standard Form 298 (Rev 2-89)
Prescribed by ANSI Std 239-18
298-102

DISCLAIMER NOTICE

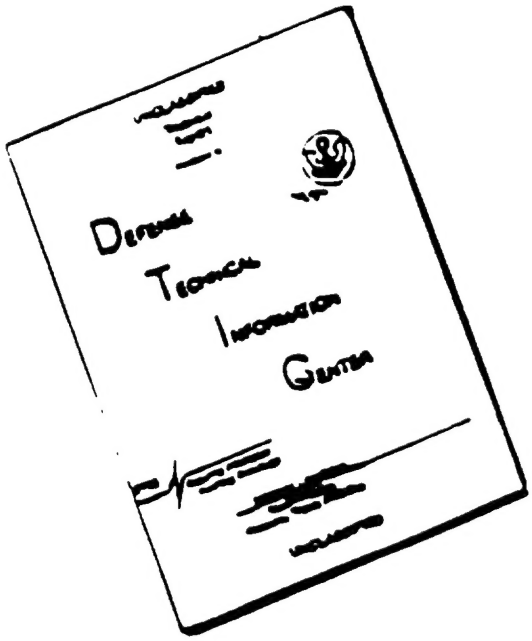

THIS DOCUMENT IS BEST QUALITY AVAILABLE. THE COPY FURNISHED TO DTIC CONTAINED A SIGNIFICANT NUMBER OF PAGES WHICH DO NOT REPRODUCE LEGIBLY.

The oxidation state of Ni in the nickel oxide electrode and related nickel oxide compounds: I. Spectroscopic evidence

H. Sambe, T.M. Nabi, and D.E. Ramaker
Chemistry Department, George Washington University, Washington, D.C. 20052

A.N. Mansour
Naval Surface Warfare Center, 10901 New Hampshire Ave., Silver Spring, MD 20903

W.E. O'Grady
Surface Chemistry Branch, Naval Research Laboratory, Washington, D.C. 20375

The electronic structures of the nickel oxide electrode, $NiO_x(OH)_{2-x}$ for x=0-1.6, and related nickel oxide materials, Li-substituted NiO, $Li_yNi_{2-y}O_2$ for y=0-1 and "Ni^{4+}" compounds, $KNiO_2(IO_4)$ and $BaNiO_3$, have been investigated using Ni 2p XPS (X-ray photoemission spectroscopy) and Ni K-edge XAS (X-ray absorption spectroscopy) data. Three aspects of the Ni 2p XPS spectra (the main peak energy, satellite energy separation, and main-line shape) and three aspects of the Ni K-edge XAS spectra (pre-edge peak energy, K-edge energy at the half-step height, and white-line peak energy) have been analyzed by the aid of simplified models and theoretical calculations. The results of these analyses consistently favor the more covalent electronic structures, $Ni^{2+}O^-_x(OH)^-_{2-x}$ [x= 1.0 and 1.5], $Li^+Ni^{2+}O^{1.5-}_2$, $K^+Ni^{2+}O^-_2(IO_4)^-$ and $Ba^{2+}Ni^{2+}O^{1.33-}_3$, over the conventional ionic electronic structures, $Ni^{(2+x)+}O^{2-}_x(OH)^-_{2-x}$ [x= 1.0 and 1.5], $Li^+Ni^{3+}O^{2-}_2$, $K^+Ni^{4+}O^{2-}_2(IO_4)^-$ and $Ba^{2+}Ni^{4+}O^{2-}_3$. This finding suggests that the oxidation of the Ni^{2+} ion is harder than oxidation of the O^{2-} anion for these nickel oxide compounds studied here.

I. INTRODUCTION

The nickel oxide electrode (NOE) has been used for over a century in nickel-cadmium batteries and therefore has been studied extensively. In spite of this effort, there still remain many questions concerning the electronic structure (ES), especially the oxidation state of Ni (OS.Ni) in the charged electrode. The overall reaction for charging of the NOE is, in the simplest form,

$$Ni(OH)_2 \rightarrow NiO_x(OH)_{2-x} + xH^+ + xe^-, \qquad (1)$$

where x can be as high as 1.6. This reaction has been interpreted as oxidation of Ni^{2+} into the higher oxidation states, Ni^{3+} and/or Ni^{4+}; that is, the oxidation product $NiO_x(OH)_{2-x}$ is viewed as

$$[Ni^{2+}_\alpha Ni^{3+}_\beta Ni^{4+}_\gamma]O^{2-}_x(OH)^-_{2-x}; \quad \alpha+\beta+\gamma=1 \text{ and } 2\alpha+3\beta+4\gamma=2+x. \quad (I)$$

Ample evidence for Ni^{3+} and Ni^{4+} species in the charged NOE have been presented by many authors [1]. The ES (I) is currently accepted by a majority of workers in the field.

On the other hand, a recent study [2, 3] by Sawatzky's group on $Li_xNi_{1-x}O$ for x=0.0-0.5 has clearly demonstrated that the ES of $Li_xNi_{1-x}O$ should be viewed as $[Li^+O^-]_x[Ni^{2+}O^{2-}]_{1-x}$ independent of x. Note that now O^{2-} rather than Ni^{2+} is oxidized, suggesting that oxidation of the Ni^{2+} ion is harder than oxidation of the O^{2-} anion for this compound. Similar phenomena have been observed for CuO and the high-temperature superconductors (such as $La_{2-x}Sr_xCuO_4$), where oxidation of Cu^{2+} has been found again to be harder than oxidation of O^{2-} [4]. The Li^+-O^- centers, normally identified with O^- ESR analysis, also appears when Li^+ ion is substituted for a metal ion in MgO, CaO, and SrO [5]. This is expected since oxidation of Mg^{2+}, Ca^{2+}, and Sr^{2+} is certainly harder than oxidation of O^{2-}. Similarly, the Na^+-O^- and K^+-O^- centers in $BaTiO_3$ appear upon

respectively substituting Na^+ and K^+ for Ba^{2+} [6], and the Al^{3+}-O^- center in $SrTiO_3$, upon substituting Al^{3+} for Ti^{4+} [7]. Finally, when an Fe ion is substituted for a Ti^{4+} in $SrTiO_3$, the Fe^{2+}-O^- center rather than the Fe^{3+}-O^- center has been observed [8], suggesting that oxidation of the Fe^{2+} ion is harder than oxidation of the O^{2-} anion for this compound. All these findings suggest that the ES of $NiO_x(OH)_{2-x}$ could be

$$Ni^{2+}O^-_x(OH)^-_{2-x} \quad \text{independent of x,} \qquad \text{(II)}$$

instead of the ES (I) above. The aim of this work is to determined which ES, (I) or (II), is closer to reality.

The nickel oxide compounds that will be studied are listed in Fig. 1 and are categorized according to the ionic oxidation state of Ni, (IOS.Ni) which is defined as the mean OS.Ni assuming the normal OS of Li^+, K^+, Ba^{2+}, O^{2-}, OH^-, and IO_4^-. This IOS.Ni is uniquely related to the composition parameters, x and y, as shown in Fig. 1. Therefore most of the figures in this paper are plotted as a function of IOS.Ni. Figure 1 includes *(a)* the NOE material, $NiO_x(OH)_{2-x}$ for x=0-2, *(b)* Li-substituted NiO, $Li_yNi_{2-y}O_2$ for y=0-1, *(c)* another battery material, $Li_{2-x}NiO_2$ for x=1-2, and *(d)* the IOS.Ni=4 compounds, $KNiO_2(IO_4)$ and $BaNiO_3$. A common property of all of these *(a)-(d)* compounds is that the Ni atom is surrounded by six oxygen atoms in a near octahedral symmetry. All compounds, except for those enclosed in dotted boxes, have a layered structure [1, 9, 10]. Both battery materials *(a)* and *(c)* are intercalation compounds of layered NiO_2 slab. In *(a)*, hydrogen atoms are intercalated between the NiO_2 slabs (i.e., intercalated into the van der Waals gap), whereas in *(c)*, Li atoms are intercalated. There is a one-to-one correspondence between these two systems in their compositions ($H_{2-x}NiO_2$ vs. $Li_{2-x}NiO_2$), but there is a key difference between them: In *(a)*, the H^+ ion is attached to a specific oxygen forming OH^-, whereas in *(c)*, the Li^+ ion sits in the middle of the van der Waals gap coordinating to six oxygen atoms, i.e., in an octahedral site of the oxygen

atoms of two NiO_2 slabs.

The nomenclature for the NOE material is as follows: The $Ni(OH)_2$ is the active material in the NOE and exists in two forms, α (hydrated) and β (anhydrous) forms. The β-NiO(OH) is the incipient oxidation product of β-$Ni(OH)_2$ in the charging process. The β-NiO(OH) notation reflects its chemical composition. When β-NiO(OH) is fully charged or overcharged, γ-"NiOOH" is produced. Here "NiOOH" does not represent its chemical composition, since γ-"NiOOH" is known to be $NiO_x(OH)_{2-x}$ with x=1.5±0.1 [11-13]. Previous assignments of the OS.Ni for the compounds in Fig. 1 are that the OS.Ni equals the IOS.Ni, except for system *(b)* where the OS.Ni=2 for y=0-1 has been proposed by Sawatzky's group [2, 3]. Our work here is to re-examine the OS.Ni=IOS.Ni assumption for the remainder of the compounds, especially for the charged NOE material, β-NiO(OH) and γ-"NiOOH".

Several experiments could differentiate the ES (I) from ES (II). Table I exhibits some of these experiments along with the associated properties that could differentiate $Ni^{3+}O^{2-}(OH)^-$ [ES (I)] from $Ni^{2+}O^-(OH)^-$ [ES (II)] for NiO(OH). We repeat, symbols of the type O^{2-}, Ni^{3+}, $(OH)^-$, etc. should be understood as the nominal valence (i.e., the OS), not as the actual atomic charge, which is in general much smaller and is not integral. The concept of the OS is useful only for ionic compounds, where the associated electron orbitals are substantially localized around an atom or a cluster of atoms. The EC specified with the OS's represents an electronic occupation for such localized orbitals. Table I is presented to clarify further the meaning of the $Ni^{3+}O^{2-}(OH)^-$ and $Ni^{2+}O^-(OH)^-$ notations. *Items (1)-(3)* utilize the difference that the O^- anion, in contrast to the closed shell ion O^{2-}, has a hole localized around the O^- anion. This difference, the presence or absence of a hole in the O^{2-}, can be used to differentiate the two EC's, $Ni^{3+}O^{2-}(OH)^-$ and $Ni^{2+}O^-(OH)^-$. *Items (4) and (5)* utilize the difference in orbital symmetry. The ground state of the Ni^{2+} and Ni^{3+} ions in the octahedral site are expected to be a high-spin $Ni^{2+}(t_{2g}^6e_g^2)\ ^3A_{2g}$

and a low-spin $Ni^{3+}(t_{2g}^6e_g)\ ^2E_g$. This difference in the orbital symmetry, ^3A and ^2E, also can be used to differentiate the two EC's. *Item (6)* utilizes the difference in the atomic charges on Ni. The Ni atomic charge for the Ni^{3+} ion is expected to be larger than that for the Ni^{2+} ion, perhaps by around 0.1 electron charge (certainly not by one). The Ni core electron binding energy is sensitive to even such a small change in the atomic charge. In this paper, paper I, we analyze the Ni XPS and Ni XAS data consisting Item (6). Items (1)-(5) and more will be discussed in the succeeding paper II.

II. Ni 2p XPS

Figure 2 shows Ni 2p XPS spectra for some of the compounds listed in Fig. 1, along with that for Ni metal. These spectra are the results obtained by Mansour's group [14]. There exist other results in the literature for Ni metal, NiO, $LiNiO_2$, and $Ni(OH)_2$. To adopt the peak energies obtained by different authors, however, great care must be taken. For example, the absolute Ni $2p_{3/2}$ peak energies for NiO obtained by Sawatzky's [3] and Mansour's [14] groups differ from each other by 1.5 eV, which is as large as the peak energy change expected for one OS number change. This discrepancy can easily arise from electrostatic charging of the sample and/or the work-function problem. We have avoided comparison of peak energies that are obtained by different authors. The widths of the peak line and energy separations between the main and satellite peaks are, on the other hand, free from the above-mentioned problems, since they are internally referenced. Below, we shall discuss the OS.Ni based upon three quantities, the Ni $2p_{3/2}$ peak energies, the satellite energy separations, and the line widths, in that order.

A. Main peak

Figure 3 plots the Ni $2p_{3/2}$ binding energies (relative to that of Ni metal) as a

function of the IOS.Ni. The solid circles represent the results obtained by Mansour's group [14], whose spectra were shown in Fig. 2. The Ni $2p_{3/2}$ peak for NiO is split as seen in Fig. 2. According to a recent study [15], this splitting originates from the Ni-Ni interaction, so that the "unperturbed" Ni $2p_{3/2}$ peak energy can be obtained by averaging the two peak energies. Accordingly, we have estimated the unperturbed peak energy for NiO. The solid and dashed lines in the figure are the expected variation of the binding energy for OS.Ni=constant (=2) and OS.Ni=IOS.Ni, respectively. These expected variations will be discussed below.

The core binding energy of a metal atom in a transition-metal compound, in general, depends upon the nature of the ligand (such as the coordination number, sizes and electronegativities of the ligand atoms) as well as the number of *d* electrons on the transition metal (i.e., the OS of the metal) and the localization of the *d* orbitals. For the samples listed in Fig. 2, however, the nature of the ligand is the same and the localization of the 3*d* orbitals are similar to each other. Consequently, the Ni $2p_{3/2}$ binding energy for those samples is predominately controlled by the OS.Ni. The Ni $2p_{3/2}$ binding energy increase per unit OS.Ni increase ($\equiv\Delta BE/\Delta OS.Ni$) can be estimated in two ways. The EC of the Ni atom in Ni metal is known to be $Ni(3d^{9.4}4s^{0.6})$, suggesting OS.Ni=0.6 [16]. From Ni metal [OS.Ni=0.6] to $Ni(OH)_2$ [OS.Ni=2.0], the Ni $2p_{3/2}$ binding energy increases by 2.8 eV. In an average, therefore, the $\Delta BE/\Delta OS.Ni$ is 2.8/(2.0-0.6) = 2.0 eV/OS. Alternatively, one can argue that the 4s electron stays around the Ni atom much closer than the oxygen 2p electrons, so that the 4s electrons should be counted with the 3d electrons, i.e., OS.Ni=0.0 for Ni metal. This argument predicts $\Delta BE/\Delta OS.Ni$ = 1.4 eV/OS. The dashed line for the OS.Ni=IOS.Ni is drawn using the lower value of 1.4 eV/OS, which gives the smaller deviation from the experimental data. When the OS.Ni=constant, the Ni 2p binding energy should be constant, as indicated by the solid line.

Increasing the OS.Ni by one, the Ni 3d electron charge should decrease by x electrons. Finding this x value gives insight into the charge redistribution with OS.Ni change. Here we estimate x from the empirical ΔBE/ΔOS.Ni values, 2.0 or 1.4 eV/OS. In a simple model, the ΔBE/ΔOS.Ni for a layered NiO_2 is given by

$$\Delta BE/\Delta OS.Ni = x[U(2p,3d) - Ae^2/4R] , \qquad (2)$$

where U(2p,3d) is the Coulomb interaction energy between the 2p and 3d electrons, R (=1.9Å) is the Ni-O distance, A (=4.71) is the Madelung constant for the CdI_2 structure [17], and e is the electron charge. The theoretical U(2p,3d) value [=F^0-G^1/15-3G^3/70] is calculated to be 36.6 eV using the F and G values in Ref. [18]. Since 80% of the theoretical value usually agrees with experiments, we adopt the U(2p,3d)=0.8×36.6 eV. Equation (2) then gives x=0.1 and 0.07 for ΔBE/ΔOS.Ni =2.0 and 1.4 eV/OS, respectively. These small x values indicate that upon OS.Ni change, the Ni 3d charge tends to remain virtually constant by readjusting the electron density between Ni and O atoms through modifying the orbital shapes. This is due to the large 3d ionization energy and the large 3d-3d interaction energy in comparison with the other interaction energies involved.

The energy difference in Fig. 3 between the dashed line and solid circles for the samples with IOS.Ni ≥3, especially for γ-"NiOOH" and $KNiO_2(IO_4)$ is much larger than possible errors in estimating the dashed-line data. This suggests the OS.Ni=2 for all three samples with IOS.Ni ≥3 and discards the conventional OS.Ni=IOS.Ni assignment. Recall that the OS.Ni=2 assignment for $LiNiO_2$ has been well established based on the oxygen K-edge XAS results by Sawatzky's group [2]. Their assignment confirms the above conclusion based on the XPS data at least for $LiNiO_2$.

We have stated above that the Ni $2p_{3/2}$ binding energy should be constant when the OS.Ni remains constant, provided that the nature of the Ni ligand is the same. For an

examination of this statement, we fortunately have a system whose OS.Ni is known and whose XPS data are available. $Li_yNi_{2-y}O_2$ for y=0-1 is such a system, which has been well established by Sawatzky's group to have OS.Ni=2 regardless of the y value and whose Ni 2p XPS spectra have been reported by the same group [3]. We have obtained the Ni $2p_{3/2}$ binding energies from their XPS spectra. The closed circles in Fig. 4 represent the Ni $2p_{3/2}$ binding energy for $Li_yNi_{2-y}O_2$ relative to that for NiO (i.e., Ni_2O_2 for y=0) as a function of the IOS.Ni [=(4-y)/(2-y)] value. The Ni $2p_{3/2}$ binding energies are indeed constant independent of the IOS.Ni value, verifying the above statement. The dashed line is, as in Fig. 3, the Ni $2p_{3/2}$ binding energies expected for OS.Ni=IOS.Ni, which are estimated using the ΔBE/ΔOS.Ni=1.4 eV/OS. The disagreement between the dashed line and the solid circles (observed energies) demotes the OS.Ni=IOS.Ni assignment and confirms the well-established OS.Ni=2 assignment for $Li_yNi_{2-y}O_2$.

B. Satellite structure

The Ni 2p peaks are accompanied by strong satellites as seen in Fig. 2. Figure 5 plots the observed energy separations between the main and satellite peaks (solid circles) as a function of the IOS.Ni. The data for the $Li_yNi_{2-y}O_2$ systems are obtained from the spectra taken by Sawatzky's group [3] and the remainder are the results by Mansour's group [14]. As mentioned earlier, these energy separations are free from electrostatic charging and/or the work-function problems. This allows us to compare the results obtained by the different groups. The energy separations are found to be around 6 eV, virtually independent of the IOS.Ni value as exhibited in the figure.

For NiO, the origin of the satellite is well understood and characterized. The electronic configuration (EC) for the ground state of NiO is $Ni^{2+}(2p^63d^8)O^{2-}(2p^6)$. Those for the Ni 2p main peak and its satellite are respectively $Ni^{2+}(2p^53d^9)O^{-}(2p^5)$ and $Ni^{3+}(2p^53d^8)O^{2-}(2p^6)$ [19]. Therefore, the energy separation between the main and

satellite peaks is given by the $3d[Ni^{2+}(2p^53d^8)]\rightarrow 2p[O^-(2p^5)]$ charge-transfer energy. The same holds for the satellite energy separation of all the compounds with OS.Ni=2. Consequently the energy separation should be constant regardless of the IOS.Ni value so long as the OS.Ni remains at 2. In other words, the OS.Ni=2 assignment for all samples presented in Fig. 5 is consistent with the observed constant energy separation.

Let us now examine the other OS.Ni=IOS.Ni ($\equiv$n) possibility. The ground-state EC would be $Ni^{n+}(2p^63d^{10-n})O^{2-}(2p^6)$. The ECs of the main and the satellite peaks would be respectively $Ni^{n+}(2p^53d^{11-n})O^-(2p^5)$ and $Ni^{(n+1)+}(2p^53d^{10-n})O^{2-}(2p^6)$. Then, the separation energy between the main and satellite peaks would be given by the $3d[Ni^{n+}(2p^53d^{11-n})]\rightarrow 2p[O^-(2p^5)]$ charge-transfer energy. It is hard to believe that this charge transfer energy could be independent of the value of n for n=2-4. In fact, we speculate without proof that the charge-transfer energy (i.e., the energy separation) could increase at least 2eV per Δn=1, as suggested in Fig. 5. [It should be larger than the ΔBE/ΔOS.Ni value (1.4 or 2.0 eV/OS) because of the presence of an extra 2p core hole at the Ni atom in comparison with the Ni 2p XPS case.] In sum, the observed constant energy separation between the main and satellite peaks (Fig. 5) is consistent with the OS.Ni=2 assignment but inconsistent with the conventional OS.Ni=IOS.Ni assignment.

C. Line width for γ-"NiOOH"

For γ-"NiOOH" (having IOS.Ni=3.5), its Ni $2p_{3/2}$ line width can be used to differentiate between the OS.Ni=2 and OS.Ni=3.5 assignments. The OS.Ni=3.5 assignment implies that some of the Ni atoms in the γ-"NiOOH" must be in the Ni^{4+} oxidation, perhaps a half in Ni^{4+} and the other half in Ni^{3+}. The Ni $2p_{3/2}$ peak energies for the Ni^{3+} and Ni^{4+} ions are expected to be separated by about 1.4-2.0 eV as discussed above. Consequently, the Ni $2p_{3/2}$ line for the OS.Ni=3.5 compound should be much broader than that for OS.Ni=2 compound, which consists of a single type of Ni ions,

namely Ni^{2+}.

In Fig. 6, the Ni $2p_{3/2}$ line shape for γ-"NiOOH" (solid circles) is compared with the line shape expected for the Ni^{2+} [solid line] and (Ni^{3+}+Ni^{4+}) [dashed line] compounds. The Ni^{2+} line shape is obtained from the α-$Ni(OH)_2$ spectrum as follows. First, the amplitude of the α-$Ni(OH)_2$ spectrum is normalized to that of the γ-"NiOOH" spectrum such that the $2p_{3/2}$ peak amplitudes agree with each other. This yielded virtually identical line shapes. By removing a smooth background, the line shapes shown in the figure are obtained for γ-"NiOOH" (solid circles) and the Ni^{2+} compound (solid line). The (Ni^{3+}+Ni^{4+}) line shape (dashed line) is constructed by superimposing the two Ni^{2+} curves whose peak energies are separated by 1.7 eV (the midpoint of the 1.4 and 2.0 eV values). These three curves are normalized at the peak energies, as seen in the figure.

Figure 6 clearly shows that the Ni $2p_{3/2}$ line shape for γ-"NiOOH" (solid circles) agrees very well with that for the Ni^{2+} compound (solid line) but disagrees with that for the (Ni^{3+}+Ni^{4+}) compound. This means that the observed line shape (or width) for γ-"NiOOH" is consistent with the OS.Ni=2 assignment but is inconsistent with the conventional OS.Ni=3.5 assignment. In summary, the line width (Fig. 6), the peak energy (Fig. 3), and the satellite separation energy (Fig. 5) for γ-"NiOOH" consistently support the OS.Ni=2 assignment.

III. Ni K-EDGE NEXAFS SPECTRA

A. Experimental results

Table II lists the energy shifts (or relative energies) of the pre-edge peak, the K-edge position, and white-line peak energy, along with the mean Ni-O bond length and the IOS.Ni value for the materials studied. These energy-shift data are obtained from Ni K-

edge NEXAFS spectra [13, 20, 21] published in the literature. Because the absolute energies are often unreliable, we have obtained the relative energies from a set of spectra appearing in the same figure or in the same table.

The pre-edge peak observed in the Ni K-edge NEXAFS data is due to a Ni($1s\rightarrow 3d$) transition. For $Ni(OH)_2$, NiO, and $KNiO_2(IO_4)$, the shape of this pre-edge feature is sharp enough to determine the peak energy, but it is too flat to do that for β-NiO(OH) and γ-"NiOOH" [21]. This is because the former materials contain only one kind of Ni site but the latter, at least two different Ni sites; for example, some Ni in γ-"NiOOH" is surrounded by two OH and four O atoms, while others are surrounded by six O atoms, The Ni K-edge energies listed in Table II are those given in Ref. [13], where the K-edge energy is defined as the energy where the intensity has half the height of the total edge jump.

The interpretation of the white line in the Ni K-edge NEXAFS data has not yet been finally established. The data listed in Table II is based on our own interpretation for the $Ni(OH)_2$ and γ-"NiOOH" data [20], which will be published separately elsewhere. Briefly, our interpretation is as follows: The white line in the $Ni(OH)_2$ data arises predominantly from multiple scattering involving the first shell of six oxygen's and can be attributed to a Ni($1s\rightarrow 4p$) transition. The NEXAFS spectra for the charged electrode (γ-"NiOOH") shows a splitting of this white line, giving a broad peak and a sharp peak [20]. The intensity of the sharp peak increases with charging and disappears when fully discharged. We attribute the broad peak to Ni site surrounded by two OH and four O atoms, and the sharp peak to Ni site surrounded by six O atoms. This sharp peak is assigned to a Ni($1s\rightarrow 4p$) transition. Accordingly, the mean Ni-O distance for this sharp peak is the same as that for Ni surrounded by six O atoms, as indicated in Table II.

The data listed in Table II, the energy shift vs. the IOS.Ni, are plotted with solid

circles in Fig. 7, along with the relative 2p binding energies presented in Fig. 3. For the 1s →3d transition, we have plotted the averaged energy of the two data. [Diamonds connected with a dashed line are theoretical results obtained with the OS.Ni=constant. These theoretical results will be discussed later.] Figure 7 exhibits a striking difference between the 2p binding energy from XPS data and the transition energies (1s→3d, K-edge, and 1s→4p) from XAS data. The binding energy is invariant against the IOS.Ni, whereas the XAS transition energies increase as the IOS.Ni increases, suggesting that the variation of the transition energies may be consistent with the OS.Ni=IOS.Ni. For γ-"NiOOH" and $KNiO_2(IO_4)$, however, this OS.Ni=IOS.Ni assignment would contradict the OS.Ni=2 conclusion based on the XPS data for these compounds.

In order to resolve this dilemma, we must consider the Ni-O bond length variation with the IOS.Ni, since they are essential to understanding the XAS data. Not only the transition energies but also the mean Ni-O bond lengths vary with the IOS.Ni as shown in Fig. 8, where the bond length data are obtained from published data in the literature [22]. The mean Ni-O bond length decreases almost linearly as the IOS.Ni increases, except for γ-"NiOOH". An accurate mean Ni-O bond length for γ-"NiOOH" is hard to determine, because the measurement must be *in situ* and is affected by self-discharging, and moreover two Ni-O bond lengths have to be determined. The large deviation from the straight line for this sample is likely due to this difficulty. Hence, the mean Ni-O bond length that is estimated from the linear relationship is likely more reliable than the experimental one. We employ this estimated mean bond length for γ-"NiOOH", which is listed in Table II and will be used for theoretical calculations later.

The variation of the mean Ni-O bond length against the IOS.Ni (Fig. 8), like that of the transition energies (Fig. 7), might also be consistent with the OS.Ni=IOS.Ni. However, this assignment for $LiNiO_2$, γ-"NiOOH", and $KNiO_2(IO_4)$ contradicts the OS.Ni=2 conclusion based on the XPS data for these compounds. [Recall also that the

OS.Ni=2 assignment for $LiNiO_2$ has been well established, based on the oxygen K-edge XAS.] In the following paper II, we will show that the OS.Ni=2 premise can account for the above-mentioned variation of the mean Ni-O bond length. This bond-length variation will be shown to arise from the increasing number of O^- ions, as the IOS.Ni value increases. Note that the increase in O^- ions there is a result of the OS.Ni=2 assignment. When the number of O^- ions increases, the covalent bonding contribution (Ni^{2+}-O^-) to the Ni-O bond increases, resulting in the shorter mean Ni-O bond length for the higher IOS.Ni compound. This suggests that the variation of the transition energies (Fig. 7) is due to the variation of the mean Ni-O bond length, which is caused by change in the covalent-bonding character (OS.Ni=2), rather than by change in the ionic-bonding character (OS.Ni=IOS.Ni). All of these will be demonstrated in the paper II.

B. Theoretical calculations

Figure 9 shows theoretical results for the transition energies (1s→3d, K-edge, and 1s→4p) and the 2p binding energies as a function of the mean Ni-O bond length. For comparison with the rest of the figures, we have also drawn an IOS.Ni scale, that is calculated from the linear relationship between the mean Ni-O bond length and the IOS.Ni, given by the dashed line in Fig. 8. These theoretical calculations are performed on NiO_6 octahedral clusters modeling the materials, where the OS.Ni (i.e., the electronic configuration for the Ni atom) is kept constant during the Ni-O bond length variation. The exitonic (1s→3d) and resonant (1s→4p) transition energies and the 2p binding energies are calculated utilizing a semi-empirical molecular orbital method. The K-edge and the white-line (1s→4p) peak energies are calculated utilizing a curved-wave multiple scattering method. Details of these calculations are described in the APPENDICES.

As mentioned above, the experimental 2p binding energy is invariant with the

IOS.Ni, whereas the experimental 1s→3d, K-edge, and 1s→4p transition energies increase as the IOS.Ni increases (see Fig. 7). This striking difference is reproduced by the theoretical results presented in Fig. 9. The origin of this difference is rather simple. The 2p binding energy involves only a core orbital (2p), whereas the 1s→3d and 1s→4p transition energies involve not only a core orbital (1s) but also a valence orbital (3d or 4p) in the final state. The core (1s and 2p) orbital energies are invariant against the variation of the mean Ni-O bond length (R), whereas the valence (e_g(3d) and t_{2u}(4p)] orbital energies increase as the R decreases, since the e_g(3d) and t_{2u}(4p) orbitals are anti-binding orbitals with respect to the Ni-O bond. Further, the 1s→4p transition energy increases faster than the 1s→3d transition energy, because the 4p atomic orbital overlaps with ligand oxygen atomic orbitals more than the 3d atomic orbital; in other words, the t_{2u}(4p) orbital is a stronger anti-binding orbital than the e_g(3d) orbital. We believe that the terminal orbital associated with the K-edge transition at the half-step height is also anti-binding and localized around a Ni atom, similar to the e_g(3d) and (4p) orbitals. This would account for the K-edge energy shift variation as a function of R.

As seen in Fig. 9, the white-line, peak-energy shifts calculated by the electron scattering method agrees well with the 1s→4p transition energy shifts calculated with the molecular orbital method. This agreement supports the conventional interpretation that the white-line peak in the Ni K-edge NEXAFS is indeed due to the Ni 1s→4p(t_{2u}) transition. However, it should be pointed out that this interpretation holds for an octahedrally coordinated Ni and not for a tetrahedrally coordinated Ni. The origin of the K-edge shift is not clear. Our NiO_6 cluster calculation results suggest that the higher shell contribution to the K-edge shift is small and that the K-edge behaves like an outer edge of the 1s→4p resonance.

The theoretical energy shifts for the OS.Ni=constant in Fig. 7 are calculated using the mean Ni-O bond lengths listed in Table II. Numerical values for the shifts are given in

Table III along with the corresponding experimental energy shifts, which show an excellent agreement with the theoretical results. In fact, most of the energy shifts are virtually identical . This agreement implies that the OS.Ni of the materials, β-NiO(OH), γ-"NiOOH", $KNiO_2(IO_4)$, and $BaNiO_3$, which appear in Table III, should be OS.Ni=2. For γ-"NiOOH" and $KNiO_2(IO_4)$, this is consistent with our conclusions on the XPS data.

What would the energy shifts be, if the OS.Ni=IOS.Ni? First of all, we estimate the transition energy increase per unit OS.Ni increase (≡ΔTE/ΔOS.Ni) using the same model as Eq. (2), which is used for the ΔBE/ΔOS.Ni estimation. In this model, the ΔTE/Δ OS.Ni for the 1s→3d transition is given by

$$\Delta TE/\Delta OS.Ni = x[U(1s,3d) - Ae^2/4R] - x[U(3d,3d) - Ae^2/4R] = x[U(1s,3d) - U(3d,3d)], \quad (3)$$

where x=0.07, which corresponds to the ΔBE/ΔOS.Ni=1.4 eV/OS. Notations for other quantities in Eq. (3) are the same as those in Eq. (2). Using the 80% of theoretical values for the Coulomb interaction integrals [18], U(1s,3d) and U(3d,3d), we obtains ΔTE/Δ OS.Ni=0.67 eV/OS for the 1s→3d transition. For $KNiO_2(IO_4)$, we have ΔOS.Ni=2 with respect to the OS.Ni=2 compound, since we are assuming OS.Ni=IOS.Ni=4 for this sample. The 1s→3d transition energy shift due to the ΔOS.Ni=2 is 2 times 0.67 eV/OS and that due to the *R* change from the IOS.Ni=2 to 4 has been estimated to be 1.8 eV (see Table III). A sum of these two contributions gives 3.1 eV. This value (3.1 eV) for the 1s →3d transition energy shift of $KNiO_2(IO_4)$ is listed in the OS.Ni=IOS.Ni column of Table III. Other energy shifts in the same column are obtained similarly, but with the following modifications. The theoretical U(4p,3d) value for the 1s→4p transition is not available [18]. So we have used the U(4s,3d) value for it. This substitution yields a smaller energy shift, so that the estimated 6.0 eV for the 1s→4p transition of γ-"NiOOH" is smaller than it should be. For the K-edge energy shifts, we have assumed that U(K,3d)≈

[U(3d,3d) + U(4s,3d)]/2, where K stands for the terminal orbital associated with the half-step-height K-edge transition. The energy shifts obtained with OS.Ni=IOS.Ni are, as seen in Table III, too large in comparison with the experimental results. In contrast, the energy shifts obtained with OS.Ni=2 agree with experiment within ±0.1 eV.

IV. CONCLUSIONS

Figures 4 - 7 and Table III summarizes our results. According to these analyses, both the XPS and XAS data favor the OS.Ni=2 assignment for the compounds studied, $LiNiO_2$, β-NiO(OH), γ-"NiOOH", $KNiO_2(IO_4)$, and $BaNiO_3$. In other words, the more covalent electronic structures, $Li^+Ni^{2+}O^{1.5-}_2$, $Ni^{2+}O^-(OH)^-$, $Ni^{2+}O^-_x(OH)^-_{2-x}$ [x=1.5], $K^+Ni^{2+}O^-_2(IO_4)^-$ and $Ba^{2+}Ni^{2+}O^{1.33-}_3$, are preferred over the conventional ionic electronic structures, $Li^+Ni^{3+}O^{2-}_2$, $Ni^{3+}O^{2-}(OH)^-$, $Ni^{(2+x)+}O^{2-}_x(OH)^-_{2-x}$ [x=1.5], $K^+Ni^{4+}O^{2-}_2(IO_4)^-$ and $Ba^{2+}Ni^{4+}O^{2-}_3$. For the fully charged nickel oxide electrode, γ-"NiOOH", three aspects of the XPS spectrum (main peak energy, satellite energy separation, and line width) and two aspects of the XAS spectrum (white-line peak energy and K-edge position), all consistently favor the OS.Ni=2 assignment. This conclusion, we believe, holds for all nickel oxide compounds whose Ni sites are octahedrally coordinated by oxygen atoms and which have a layered or chain structure, but may not hold for the compounds which have a 3-dimensional networked structure, such as a rutile or fluorite structure.

ACKNOWLEDGMENTS

The authors gratefully acknowledge the support of the Office of Naval Research.

APPENDIX A: Molecular Orbital calculations

We are concerned here with the R dependence of the transition energies for a relatively small variation (≤0.2Å) of R (≡the Ni-O bond length). This makes the theoretical calculations much easier, because we can avoid calculation of the multiplet splitting, which, in comparison with the orbital energies of the antibonding orbitals, is insensitive to a small change of R. Consequently the R dependence of a state (arising from an electronic configuration) or the slope of energy against R is approximately equal to the R dependence of the average energy of the multiplets arising from the electronic configuration. This means that we can use simple models, such as Hyper Hartree-Fock or Xα [23], whose total energy is an average of the multiplet energies, to evaluate the R dependence of the transition energies.

In an octahedral ligand field, the Ni 3d orbital is split into the t_{2g} and e_g components, and the Ni 4p orbital has t_{2u} symmetry. For the $Ni^{2+}(3d^8)$ anion, the electronic configuration is $Ni^{2+}(t_{2g}^6\, e_g^2\, t_{2u}^0)$. The Ni(1s→3d) and Ni(1s→4p) transitions should be written as Ni(1s→e_g) and Ni(1s→t_{2u}), but we shall keep the atomic notation. In the Xα method [23], the Ni 2p binding energy and the Ni(1s→3d) and Ni(1s→4p) transition energies are given by

$$\begin{aligned} &\text{Ni 2p binding energy:} && \text{BE(2p)} = -\varepsilon_{2p} \\ &\text{Ni(1s→3d) transition energy:} && \text{TE(1s→3d)} = \varepsilon_{eg} - \varepsilon_{1s} \\ &\text{Ni(1s→4p) transition energy:} && \text{TE(1s→4p)} = \varepsilon_{t2u} - \varepsilon_{1s}' \end{aligned} \qquad \text{(A1)}$$

where the orbital energies, ε_i, are calculated with the intermediate electronic configuration (namely with "the transition state procedure" [23] which includes the electronic relaxation). The Ni 1s orbital energies, ε_{1s} and ε_{1s}', for the 1s→3d and 1s→4p transitions are different, because the intermediate electronic configurations for the two transitions are different.

The R dependence of BE(2p), TE(1s→3d), and TE(1s→4p) are given by the expressions,

$$\begin{aligned} \text{BE(2p)} &= -[\varepsilon_{2p}(R) - \varepsilon_{2p}(R_0)] \\ \text{TE(1s→3d)} &= [\varepsilon_{eg}(R) - \varepsilon_{eg}(R_0)] - [\varepsilon_{1s}(R) - \varepsilon_{1s}(R_0)] \\ \text{TE(1s→4p)} &= [\varepsilon_{t2u}(R) - \varepsilon_{t2u}(R_0)] - [\varepsilon_{1s}'(R) - \varepsilon_{1s}'(R_0)] \end{aligned} \qquad \text{(A2)}$$

where R_0=2.07Å, the Ni-O bond length of the IOS.Ni=2 compounds. Core orbital energies, $\varepsilon_{2p}(R)$, $\varepsilon_{1s}(R)$, and $\varepsilon_{1s}'(R)$, are almost invariant against a small variation of R, so long as the electronic configuration, $t_{2g}^6 e_g^2$, is kept independent of R. In other words, if the OS.Ni (i.e., number of 3d electrons in Ni) is kept constant, the R dependencies are approximately given by

$$\begin{aligned} \text{BE(2p)} &\approx 0 \\ \text{TE(1s→3d)} &\approx \varepsilon_{eg}(R) - \varepsilon_{eg}(R_0) \\ \text{TE(1s→4p)} &\approx \varepsilon_{t2u}(R) - \varepsilon_{t2u}(R_0) \end{aligned} \qquad \text{(A3)}$$

The theoretical energy shifts for the Ni 2p binding energies are therefore BE(2p)=0, as indicated in Fig 9. The R dependencies (A3) are rather insensitive to the actual electronic configuration used in the calculation, so long as the EC is kept the same.

We now evaluate the $\varepsilon_{eg}(R)$ and $\varepsilon_{t2u}(R)$ orbital energies keeping the electronic configuration constant. The R dependence of the orbital energies for antibonding orbitals, such as e_g and t_{2u}, can be reproduced rather accurately using practically any method which includes the overlapping effect of the atomic orbitals. We have used the extended Hückel method with the code supplied by Hyper Chem [24] for an octahedral NiO_6 cluster modeling the materials. To keep the electronic configuration constant, we have performed the calculations without charge iteration for all R. We have examined the effect of nuclear-geometry distortions, such as long and short Ni-O distances for β-NiO(OH) and

angular distortions between Ni-O bonds. The effects of the distortions on the calculated orbital energies are found to be negligibly small. The extended Hückel orbital energies for the perfect octahedral NiO_6 are used to calculate the 1s→3d and 1s→4p transitions (A3). The resulting transition energies are plotted in Fig. 9 as the molecular orbital results (solid circles).

APPENDIX B: Electron Scattering Calculations

The Ni K-edge NEXAFS spectra, revealing the K-edge position and white-line peak, can be directly calculated using a multiple-scattering method such as the one used in the FEFF6 code [25]. The FEFF6 calculations are performed on a perfect octahedral cluster of NiO_6 including a large number of multiple scattering paths (LEG=8). We have implicitly kept the electronic configuration constant by utilizing the same atomic electron densities for all *R*, that is, by not assigning atomic charges in the input data. The resulting Ni K-edge NEXAFS spectra agree well with the corresponding experimental spectra. The theoretical *R* dependence of the white-line peak positions (i.e., the first peak energies) are shown in Fig. 9 as solid diamonds and labeled as 1s→4p. The effect of distortion of the nuclear-geometry has been found to be larger in the FEFF6 calculations than in the extended Hückel calculations. Nevertheless, the distortion effect is small enough to be ignored.

To calculate the K-edge, half-step-height energies, we have employed two definitions for the step height; (i) the "atomic" absorption μ_0 amplitude at 100 eV above the threshold energy and (ii) the first peak amplitude in μ_0. These two definitions introduce a negligible difference for the calculated K-edge shifts. The effect of distortion of the nuclear-geometry on the K-edge energy is found to follow closely the distortion effect on the white-line energy. The K-edge shifts for a perfect octahedral NiO_6 are shown in Fig. 9 with solid diamonds along with other theoretical results.

The origin of the K-edge shift is not clear. We are not aware of any explanation in the literature, except the statement that the K-edge shift is due to the change in oxidation state of the absorbing atom. As mentioned above, we believe that the white-line peaks in our samples originate from the 1s→4p transition. However, we are not sure what controls the energy position of the K-edge as defined by the half-step height. Intuitively we expect that μ_0, which depends on not only the absorbing Ni atom but also on the neighboring atoms, might control the K-edge shift. Another possibility is that the 1s→4p transition, through the χ, influences the absorption, μ ($=\mu_0 + \chi\mu_0$) in the edge region. We have calculated the K-edge shift for μ_0 and found that the μ_0 contribution to the K-edge shift contributes only about 28%, indicating that the χ essentially controls the size of the K-edge shift. This finding and a linear relation between the K-edge shifts and the 1s→4p transition energies (see Fig. 9) suggest that the K-edge shift, like the white-line peak shift, is largely controlled by the 1s→4p transition. The white-line peak, however, can be affected by higher shells containing heavy atoms such as the case for $BaNiO_3$, whereas the K-edge shift will be affected less by the higher shell so that it can reflect the 1s→4p transition even when the higher shell contribution is large. This is certainly an advantage of utilizing the K-edge shift over the white-line shift to trace the 1s→4p transition, for octahedrally coordinated Ni.

REFERENCES

[1] See review articles: P. Oliva, J. Leonardi, J.F. Laurent, C. Delmas, J.J. Braconnier, M. Figlarz, F. Fievet, and A. de Gulbert, J. Power Source **8**, 229 (1982); J. McBreen, in *Modern Aspects of Electrochemistry*, edited by R.E. White, J. O'M. Bockris, and B.E. Conway (Plenum, New York, 1990), **No. 21**, p. 29.

[2] P. Kuiper, G. Kruizinga, J. Ghijsen, and G.A. Sawatzky, Phys. Rev. Lett. **62**, 221 (1989).

[3] J. van Elp, H. Eshes, P. Kuiper, and G.A. Sawatzky, Phys. Rev. **B 45**, 1612 (1992).

[4] S. Hüfner, *Photoelectron Spectroscopy* (Springer-Verlag, Berlin, 1995), p. 205-229.

[5] O.F. Schirmer, J. Phys. Chem. Solids **32**, 499 (1971).

[6] T. Varnhorst et al., Phys. Rev. **B 53**, 116 (1996).

[7] O.F. Schirmer, W. Berlinger, and K.A. Müller, Solid State Commun. **18**, 1505 (1976).

[8] Th.W. Kool and M. Glasbeek, J. Phys. Condens. Matter **5**, 361 (1993).

[9] C. Delmas, Mat. Res. Soc. Symp. Proc. **293**, 15 (1993).

[10] T. Ohzuku, A. Ueda, and M. Nagayama, J. Electrochem. Soc. **140**, 1862 (1993).

[11] D.A. Corrigan and S.L. Knight, J. Electrochem. Soc. **136**, 613 (1989).

[12] T.W. Capenhart et al., Appl. Phys. Lett. **58**, 865 (1991).

[13] K.I. Pandya, K.E. Swider, D.A. Corrigan, and W.E. O'Grady, J. Electrochem. Soc. ****(1996).

[14] Mansour's XPS paper

[15] M.A. van Veenendaal and G.A. Sawatzky, Phys. Rev. Lett. **70**, 2459 (1993).

[16] Ni metal 3d**4s** electronic structure

[17] L. Pauling, *The Nature of the Chemical Bond* (Cornell University Press, Ithaca, 1960), Third Edition, p. 508.

[18] J.B. Mann, Los Alamos Scientific Laboratory Report **NO. LA-3690**, 1967.

[19] S. Hüfner, *Photoelectron Spectroscopy* (Springer-Verlag, Berlin, 1995), p. 185.

[20] J. McBreen et al., J. Phys. Chem. **93**, 6308 (1989).

[21] A.N. Mansour, C.A. Melendres, M. Pankuch, and R.A. Brizzolara, J. Electrochem. Soc. 141, L69 (1994); A.N. Mansour and C.A. Melendres, The Electrochem. Soc. Extended Abstracts Vol. **2**, 229 (1994).

[22] See the following paper, paper II, for the references.

[23] J.C. Slater, *The Self-consistent Field for Molecules and Solids: Quantum Theory of Molecules and Solids* Vol. 4 (McGraw-Hill, New York, 1974).

[24] HyperChem (trademark) Release 3 for Windows (Autodesk, Inc., Sausalito, CA, 1993).

[25] J. Mustre de Leon, J.J. Rehr, S.I. Zabinsky, and R.C. Albers, Phys. Rev. **B 44**, 4146 (1991); J.J. Rehr, Japan. J. Appl. Phys. **Supp. 32**, 8 (1993).

FIGURE CAPTIONS

FIG. 1. Three series of nickel oxide compounds listed according to the IOS.Ni. All compounds consist of NiO_6 octahedrons and have, except for those enclosed in dotted boxes, a layered structure. Relationships between the IOS.Ni (≡n) and the chemical composition parameters, x and y, are indicated.

FIG. 2. Ni 2p XPS spectra for some of nickel oxide compounds listed in Fig. 1 along with that for Ni metal.

FIG. 3. Ni $2p_{3/2}$ binding energy as a function of the IOS.Ni. The solid and dashed lines are the expected variations of the binding energy for OS.Ni=constant and OS.Ni=IOS.Ni, respectively.

FIG. 4. Ni $2p_{3/2}$ binding energy for $Li_yNi_{2-y}O_2$ (y=0.0-0.8) [Ref. 3] vs. the IOS.Ni [≡n=(4-y)/(2-y)]. The solid and dashed lines are the expected variations of the binding energy for OS.Ni=constant and OS.Ni=IOS.Ni, respectively.

FIG. 5. Energy separation between the main and satellite peaks of Ni $2p_{3/2}$ as a function of the IOS.Ni. The solid and dashed lines are the expected variations of the energy separation for OS.Ni=constant and OS.Ni=IOS.Ni, respectively.

FIG. 6. The Ni $2p_{3/2}$ line shape for γ-"NiOOH" (solid circles). The solid and dashed lines are the expected line shapes for the Ni^{2+} and (Ni^{3+}+Ni^{4+}) compounds, respectively.

FIG. 7. Pre-edge peak (1s→3d), edge position (K-edge), and white-line peak (1s→4p) energies of Ni K-edge NEXAFS spectra [Table II] (solid circles and solid lines) plotted as a function of the IOS.Ni, along with the 2p binding energies. Mean energies for the IOS.Ni=2 compounds are set to zero for all four cases. Diamonds and dashed lines are the transition energies calculated with OS.Ni =constant.

FIG. 8. Mean Ni-O bond length vs. the IOS.Ni. The dashed straight line indicates an trend in the variation of the bond length as a function of the IOS.Ni. A large deviation from the straight line for γ-"NiOOH" is likely due to experimental difficulty (see the text).

FIG. 9. Theoretical 1s→3d, K-edge, 1s→4p, and 2p-binding energies of a NiO_6 cluster calculated as a function of the Ni-O bond length with OS.Ni=constant. The IOS.Ni scale is calculated from the linear relationship between the mean Ni-O bond length and the IOS.Ni, which is shown with the dashed line in Fig. 8. Two theoretical approaches, molecular orbital (solid circles) and electron scattering (solid diamonds), are used.

Table I. Experiments and associated physical properties that could differentiate the $Ni^{3+}O^{2-}(OH)^-$ from $Ni^{2+}O^-(OH)^-$ electronic configuration for NiO(OH).

		Electronic configuration	
Property	Experiment	$Ni^{3+}O^{2-}(OH)^-$	$Ni^{2+}O^-(OH)^-$
1s(O) → 2p(O) transition	Oxygen K-edge XAS	Absent	Present
3d(Ni) → 2p(O) transition	Optical absorption	Absent	Present
Electron conduction in the oxygen 2p band	Photoelectron current	Absent	Present
Jahn-Teller distortion	X-ray diffraction EXAFS	Present	Absent
Magnetic moment	Magnetic susceptibility	due to Ni^{3+}	Ni^{2+} and O^-
Ni atomic charge	Ni XPS and Ni XAS	Larger than $Ni^{2+}(OH)^-_2$	Same as

Table II. Energy shifts of the white-line peak, the K-edge, and the pre-edge peak obtained from Ni K-edge NEXAFS results in the literature, Refs. [20], [13], and [21] respectively, along with the mean Ni-O distances.

Transition	Compound	IOS.Ni	Mean Ni-O distance (Å)	Energy shift (eV)
White-line peak (1s → 4p)	β-$Ni(OH)_2$	2	2.07	0.0
	γ-"NiOOH"	3.5	1.88[a)]	3.9
K-edge position (at a half height)	β-$Ni(OH)_2$	2	2.07	0.0
	β-NiO(OH)	3	1.96	1.4
	γ-"NiOOH"	3.5	1.92[b)]	2.3
	$BaNiO_3$	4	1.86	3.0
Pre-edge peak (1s → 3d)	α-$Ni(OH)_2$	2	2.05	0.0
	$KNiO_2(IO_4)$	4	1.88	2.0
	NiO	2	2.09	0.0
	$KNiO_2(IO_4)$	4	1.88	1.7

[a)] Mean Ni-O for Ni surrounded by 6 oxygen atoms (see the text).

[b)] Estimated from the linear relation between the mean Ni-O and the IOS.Ni shown in Fig. 8 (see the text).

Table III. Comparison of the experimental energy shifts (from Table II) with the theoretical energy shifts obtained assuming OS.Ni=2 or OS.Ni=IOS.Ni. The energy shifts are referred to the IOS.Ni=2 compounds, α-$Ni(OH)_2$, β-$Ni(OH)_2$, or NiO.

Transition	Compound	Energy shift (eV)		
		Experimental	OS.Ni = 2	OS.Ni = IOS.Ni
1s → 4p	γ-"NiOOH"	3.9	3.8	6.0
K-edge	β-NiO(OH)	1.4	1.5	2.6
	γ-"NiOOH"	2.3	2.2	3.9
	$BaNiO_3$	3.0	3.0	5.2
1s → 3d	$KNiO_2(IO_4)$	1.85	1.8	3.1
2p binding energy	$LiNiO_2$	0.17	0.0	1.4
	γ-"NiOOH"	-0.13	0.0	2.1
	$KNiO_2(IO_4)$	-0.03	0.0	2.8

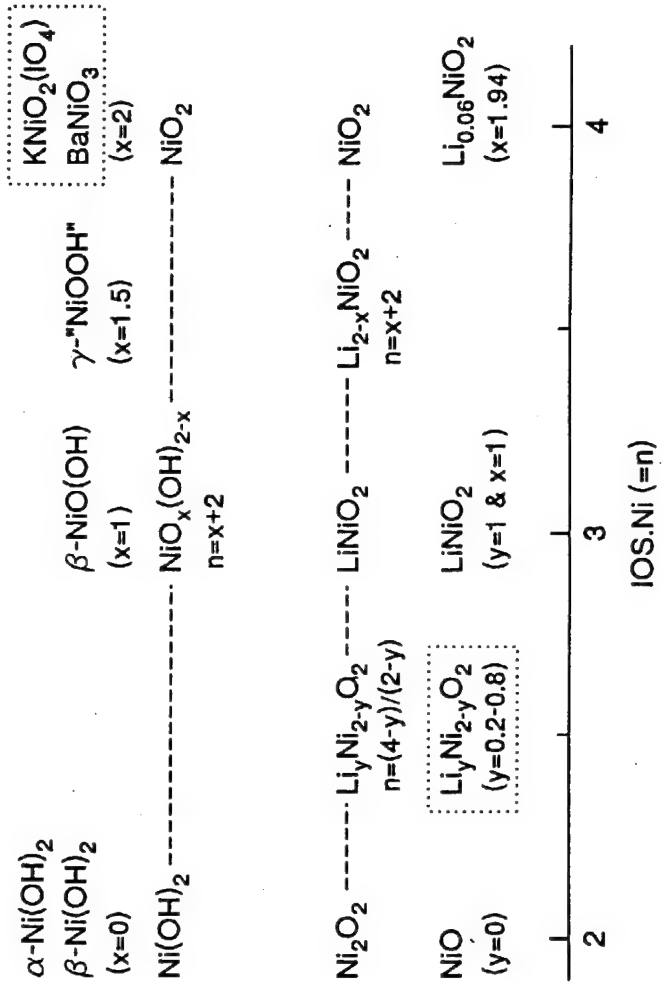

Fig. 1

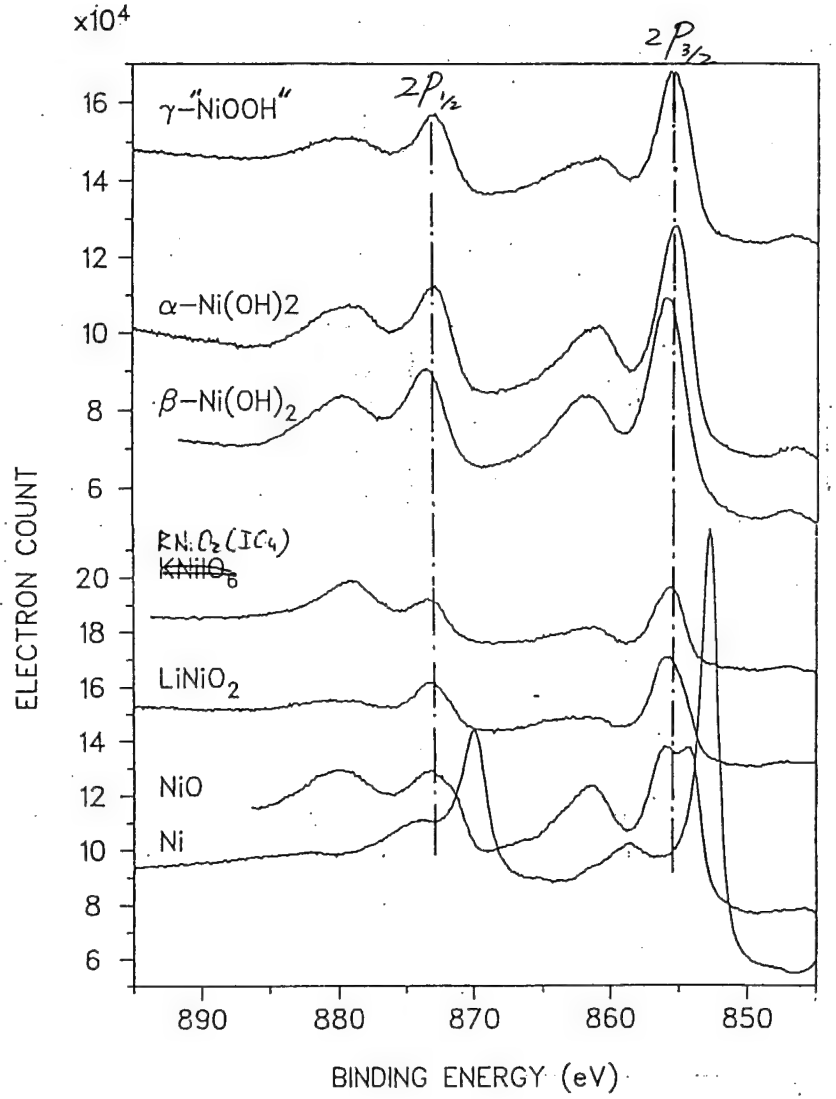
XPS SPECTRA OF Ni 2p
x10⁴
2p3/2
2p1/2
γ-"NiOOH"
α-Ni(OH)2
β-Ni(OH)2
KNiO2(IO4)
KNiO6
LiNiO2
NiO
Ni
ELECTRON COUNT
BINDING ENERGY (eV)
890
880
870
860
850

Fig. 2

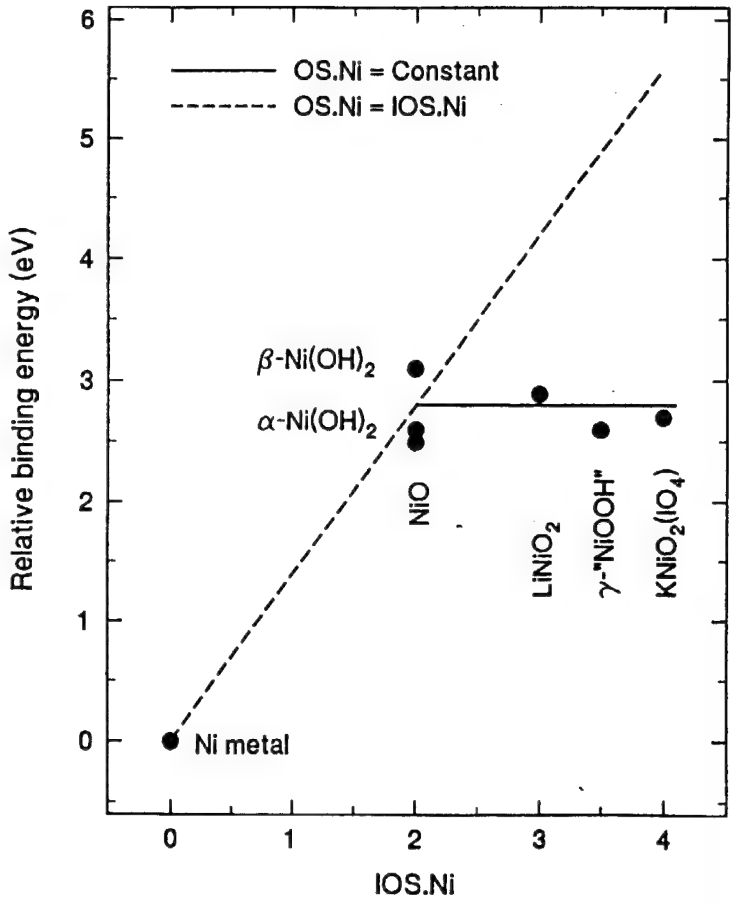
OS.Ni = Constant
OS.Ni = IOS.Ni
β-Ni(OH)2
α-Ni(OH)2
NiO
LiNiO2
γ-"NiOOH"
KNiO2(IO4)
Ni metal
Relative binding energy (eV)
IOS.Ni

Fig. 3

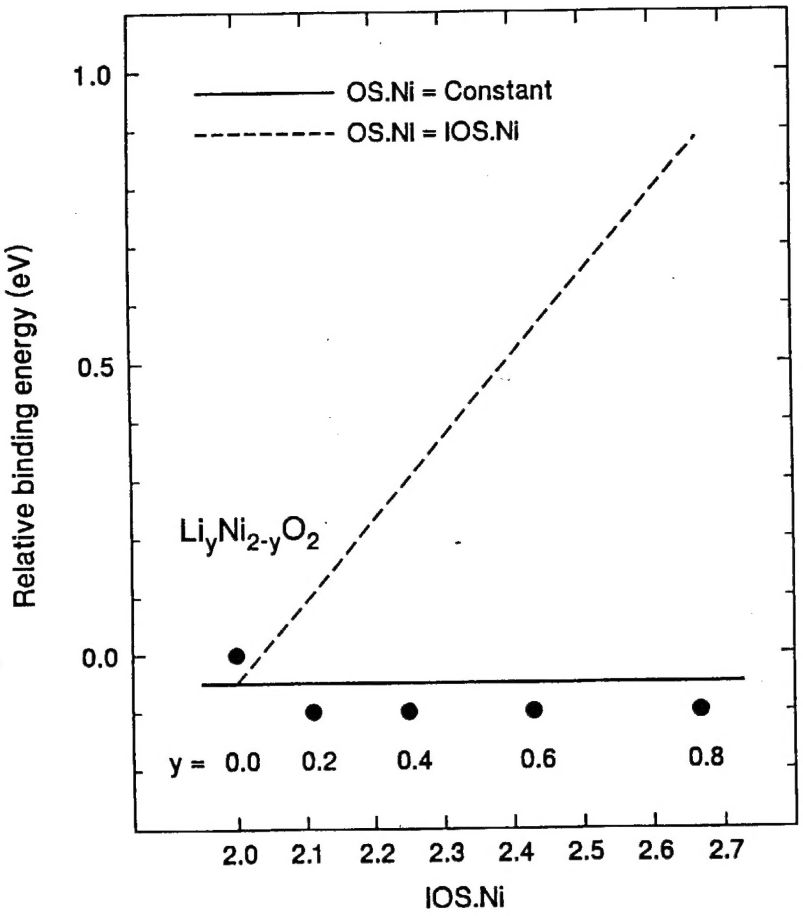
OS.Ni = Constant
OS.Ni = IOS.Ni
$Li_yNi_{2-y}O_2$
y = 0.0 0.2 0.4 0.6 0.8
Relative binding energy (eV)
1.0
0.5
0.0
2.0 2.1 2.2 2.3 2.4 2.5 2.6 2.7
IOS.Ni

Fig. 4

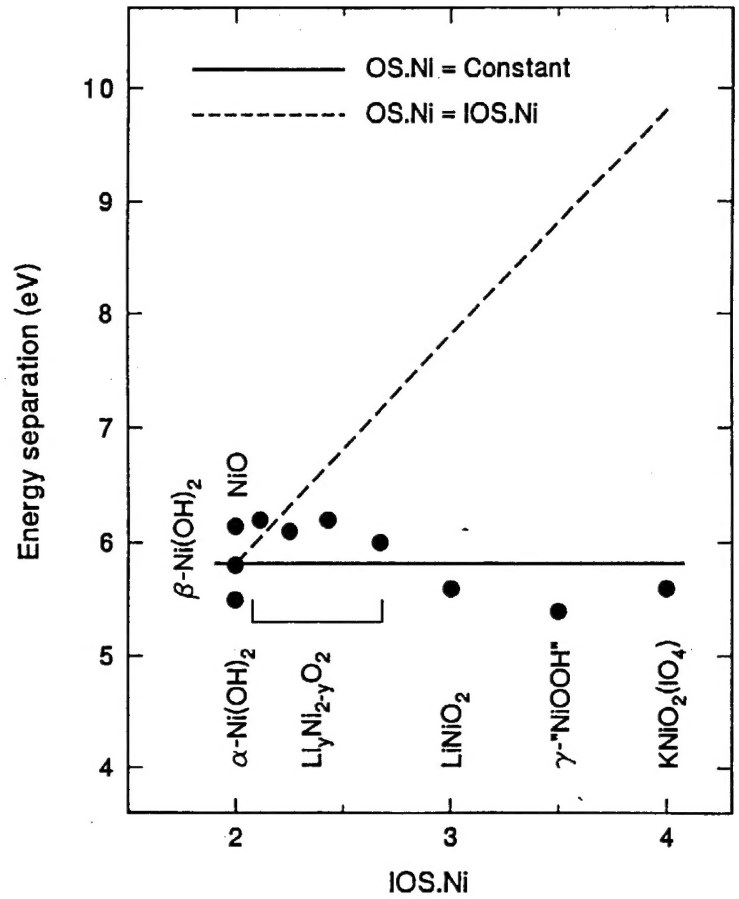
OS.Ni = Constant
OS.Ni = IOS.Ni
Energy separation (eV)
10
9
8
7
6
5
4
β-Ni(OH)$_2$
NiO
α-Ni(OH)$_2$
$Li_yNi_{2-y}O_2$
$LiNiO_2$
γ-"NiOOH"
$KNiO_2(IO_4)$
2
3
4
IOS.Ni

Fig. 5

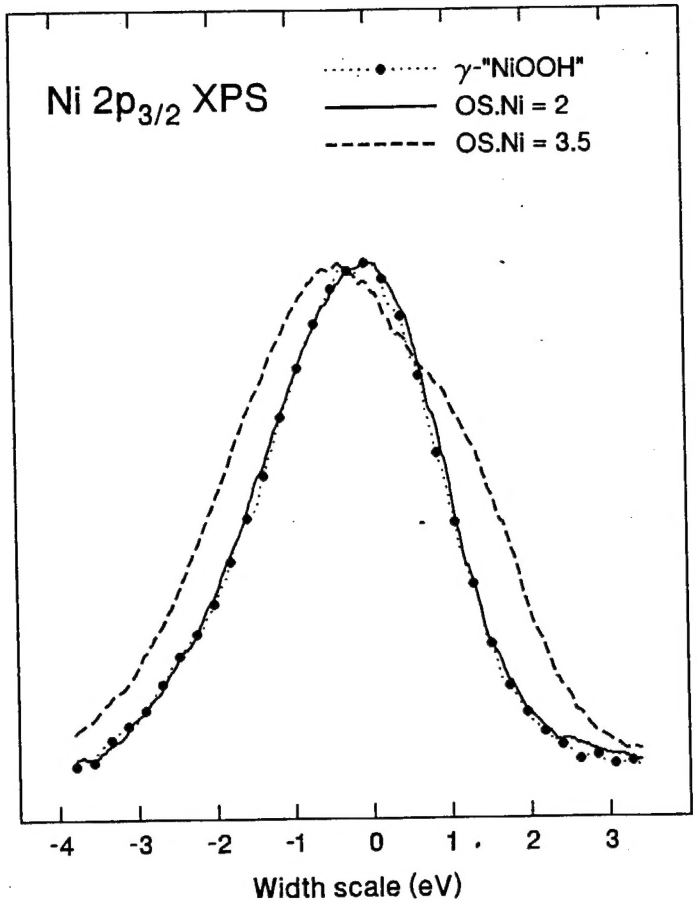
Ni 2p3/2 XPS
γ-"NiOOH"
OS.Ni = 2
OS.Ni = 3.5
-4
-3
-2
-1
0
1
2
3
Width scale (eV)

Fig. 6

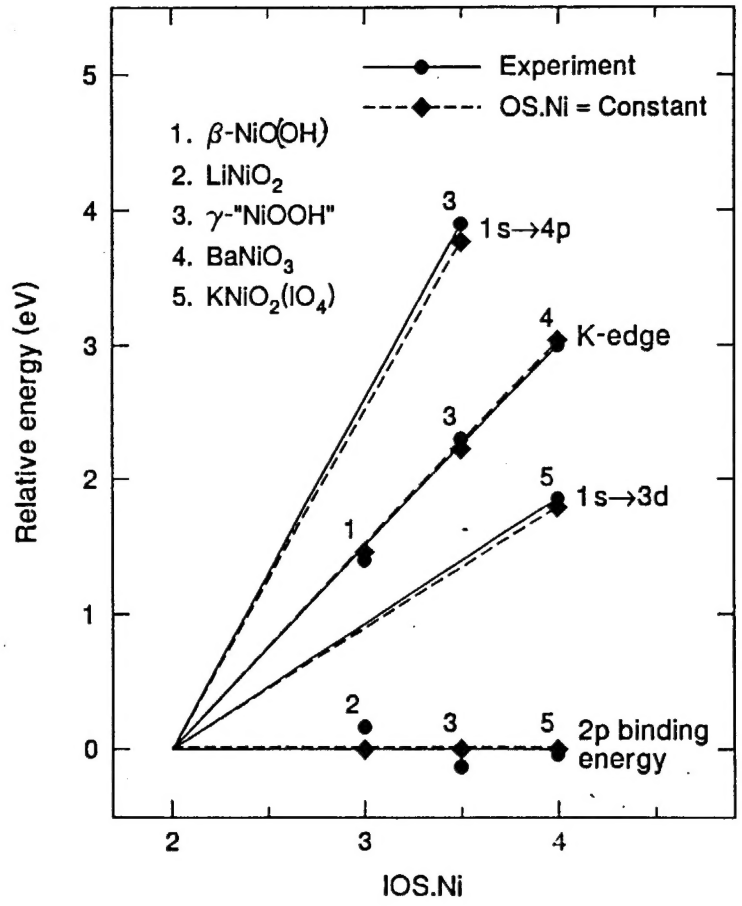
Experiment
OS.Ni = Constant
1. β-NiO(OH)
2. LiNiO2
3. γ-"NiOOH"
4. BaNiO3
5. KNiO2(IO4)
1s→4p
K-edge
1s→3d
2p binding energy
Relative energy (eV)
IOS.Ni
0
1
2
3
4
5

Fig. 7

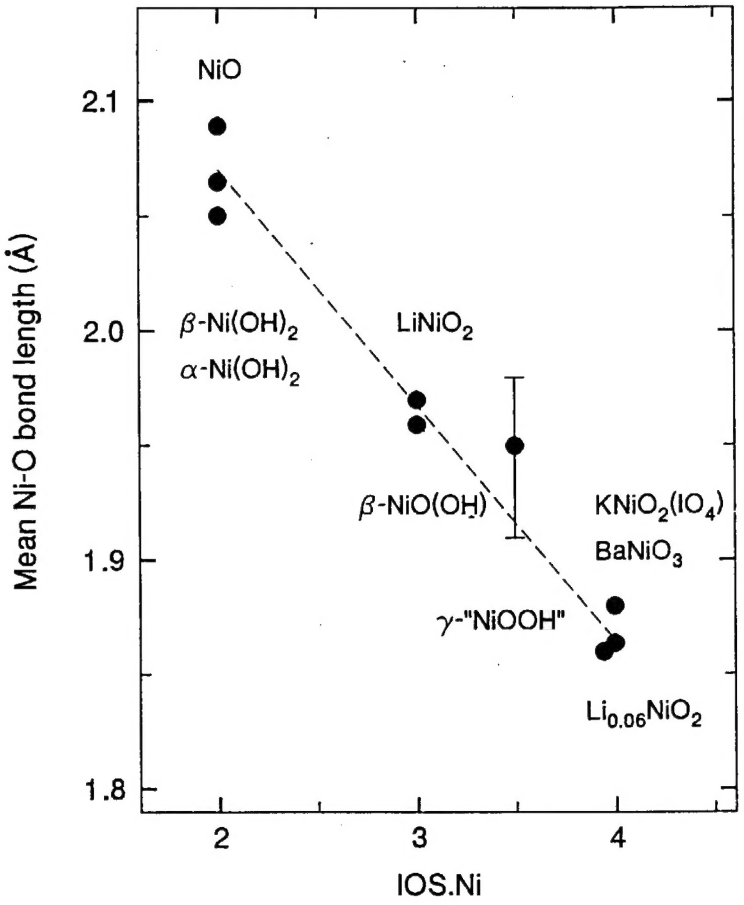
NiO
2.1
2.0
1.9
1.8
β-Ni(OH)2
α-Ni(OH)2
LiNiO2
β-NiO(OH)
KNiO2(IO4)
BaNiO3
γ-"NiOOH"
Li0.06NiO2
Mean Ni-O bond length (Å)
2
3
4
IOS.Ni

Fig. 8

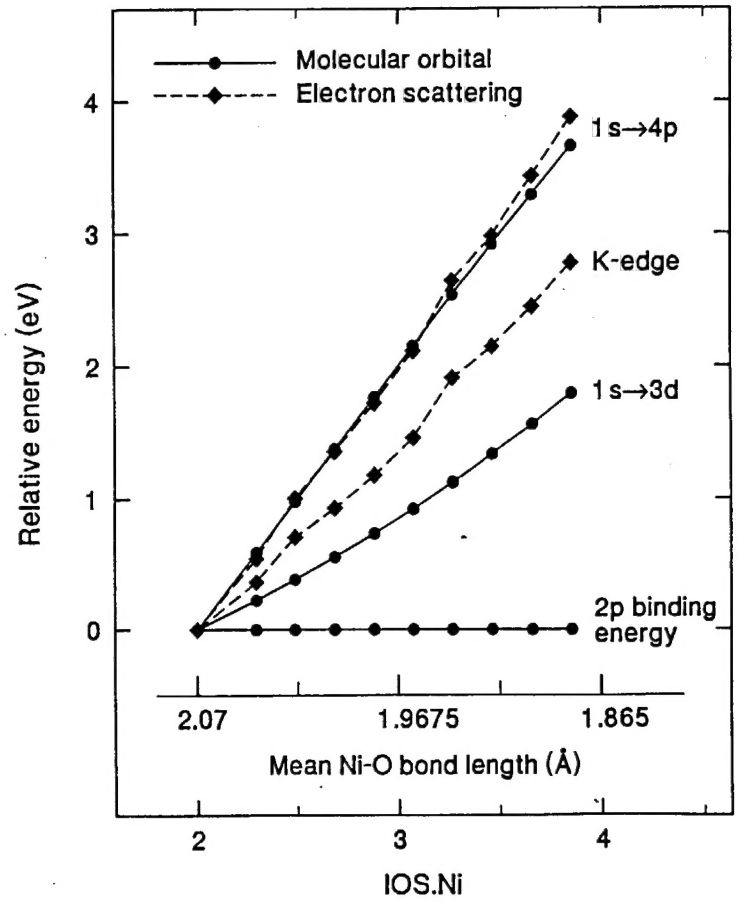
Molecular orbital
Electron scattering
1s→4p
K-edge
1s→3d
2p binding energy
Relative energy (eV)
4
3
2
1
0
2.07
1.9675
1.865
Mean Ni-O bond length (Å)
2
3
4
IOS.Ni

Fig. 9

Technical Report Distribution List

Dr. Robert J. Nowak (1)*
ONR 331
800 N. Quincy St.
Arlington, VA 22217-5660

Defense Technical Information Ctr (2) **
Building 5, Cameron Station
Alexandria, VA 22314

Dr. James S. Murday (1)
Chemistry Division, NRL 6100
Naval Research Laboratory
Washington, DC 20375-5660

Dr. John Fischer (1)
Chemistry Division, Code 385
NAWCWD - China Lake
China Lake, CA 93555-6001

Dr. Peter Seligman (1)
NCCOSC - NRAD
San Diego, CA 92152-5000

Dr. James A. Gucinski (1)
NSWC Code 609
300 Highway 361
Crane, IN 47522-5001

Mr. Christopher Egan (1)
Naval Undersea Warfare Center
Division Newport
1176 Howell St.
Newport, RI 02841-1708

Dr. Carl Mueller
Naval Surface Warfare Center - White Oak
Code R36
10901 New Hampshire Ave.
Silver Spring, MD 20903-5640

* Number of copies required